

PointDiffuse: A Dual-Conditional Diffusion Model for Enhanced Point Cloud Semantic Segmentation

Yong He¹, Hongshan Yu^{2*}, Mingtao Feng³, Tongjia Chen⁴, Zechuan Li²,
Anwaar Ulhaq⁵, Saeed Anwar⁶, Ajmal Saeed Mian⁴

¹Anhui University, ²Hunan University, ³Xidian University,

⁴University of Western Australia, ⁵Central Queensland University, ⁶Australian National University,

Abstract

Diffusion probabilistic models are traditionally used to generate colors at fixed pixel positions in 2D images. Building on this, we extend diffusion models to point cloud semantic segmentation, where point positions also remain fixed, and the diffusion model generates point labels instead of colors. To accelerate the denoising process in reverse diffusion, we introduce a noisy label embedding mechanism. This approach integrates semantic information into the noisy label, providing an initial semantic reference that improves the reverse diffusion efficiency. Additionally, we propose a point frequency transformer that enhances the adjustment of high-level context in point clouds. To reduce computational complexity, we introduce the position condition into MLP and propose denoising PointNet to process the high-resolution point cloud without sacrificing geometric details. Finally, we integrate the proposed noisy label embedding, point frequency transformer and denoising PointNet in our proposed dual conditional diffusion model-based network (PointDiffuse) to perform large-scale point cloud semantic segmentation. Extensive experiments on five benchmarks demonstrate the superiority of PointDiffuse, achieving the state-of-the-art mIoU of 74.2% on S3DIS Area 5, 81.2% on S3DIS 6-fold and 64.8% on SWAN dataset.

1. Introduction

Point cloud segmentation is a fundamental 3D vision task supporting a wide range of applications in autonomous driving [31, 54], and robotics [6, 36]. Semantic segmentation methods have evolved from early MLP-based methods [8, 21, 30] that apply MLPs on points to model local point features, to convolution-based methods [12, 38] that learn convolutional weights to model local point connections. More recently, transformer-based methods [13, 46] have been proposed to incorporate the attention mechanism to learn contextual information.

However, raw point clouds captured by depth sensors

or LiDARs are often contaminated with noise due to environmental factors or sensor limitations. While local aggregation methods exhibit strong representational capabilities, they remain vulnerable to noise, particularly at object boundaries and in small object regions. Consequently, the denoising limitations of existing segmentation methods can lead to suboptimal performance in these challenging areas. Recently, the Diffusion Probabilistic Model (DPM) [14] has gained popularity as a powerful class of generative models capable of generating high-quality and diverse images. DPMS have an inherent denoising capability. Motivated by its success, many researchers have applied DPMS in several other 2D computer vision tasks, such as image segmentation [45, 49], and object detection [2, 4]. Diffusion models have also been gradually extended to 3D computer vision tasks such as shape generation [26, 58], shape completion [5, 59], 3D detection [15], and 3D part segmentation [48]. Diffusion models are particularly effective at handling noise, given their strong denoising capabilities. Compared to traditional local aggregation networks, diffusion models offer two key advantages:

- *Enhanced flexibility:* Diffusion models exhibit enhanced flexibility and can generate diverse predictions through multiple runs. This is akin to test-time augmentation, as demonstrated in [18], where diverse predictions are combined to produce better segmentation.
- *Improved adaptability:* Multiple runs of generative models enable them to adapt to different scenarios or data distributions, improving their generalization ability.

Given the above advantages, we argue that diffusion models are particularly well-suited for handling noisy point cloud data characterized by intricate contextual connections. Motivated by this, we endeavor to leverage diffusion for large-scale point cloud segmentation. However, using diffusion models for this task is not straightforward and faces the following challenges.

- *Long runtime:* Generating large-scale point labels requires a large number of denoising steps in the reverse diffusion process, leading to extended inference time.

- *Limited local denoising ability*: The ability of diffusion models to handle local noise is somewhat restricted when processing unordered and irregular points.
- *Loss of fine-grained features*: The diffusion model may overly smooth the label distribution, leading to the loss of subtle semantic features.

To overcome the aforementioned challenges, we propose a dual conditional diffusion network for point cloud segmentation, coined **PointDiffuse**. Our key idea involves integrating dual conditions (i.e., semantic and position conditions) and local aggregation into the diffusion model. Specifically, **i**) we design a noisy embedding layer for low-level geometric denoising, which performs convolution operations on noisy features. The convolutional weights are learned from the semantic condition and used to mask the noise based on the position condition. By anchoring the noise using dual conditions, the diffusion model obtains a preliminary semantic reference, facilitating the rapid generation of point labels while suppressing the loss of fine-grained features. **ii**) We propose a point frequency transformer for high-level context denoising. The point frequency transformer converts the noise features and position conditions from the spatial to the frequency domain and then uses vector attention on these features to learn context connections. The diffusion model achieves position awareness by introducing the position condition in the transformer to improve the local denoising ability. **iii**) Furthermore, to decrease the long runtime, we propose a simple but efficient Denoising PointNet over the high resolution point clouds that introduces the position condition into MLP. In summary, our contributions are:

- We propose *PointDiffuse*, a dual conditional diffusion model for large-scale point cloud segmentation.
- We propose a *Noisy Label Embedding* mechanism that integrates semantic and local position conditions to stabilize variance in the diffusion process.
- We propose a *Point Frequency Transformer* that adaptively filters out noise, enhancing segmentation quality.
- We develop a simple yet effective *Denoising PointNet* to improve the overall computational efficiency.

To demonstrate the effectiveness of our proposed method, we conduct extensive experiments on five benchmark datasets: S3DIS [1], ScanNet [7], SWAN [17], SemanticKITTI [3], and ShapeNet [53]. Without relying on multi-dataset or multi-modal joint training, our method achieves state-of-the-art performance with 74.2% and 81.2% mIoU on S3DIS Area 5 and 6-fold cross-validation for indoor semantic segmentation, and 64.8% mIoU on SWAN for outdoor semantic segmentation. It also achieves competitive performance of 88.4% Ins. mIoU on ShapeNet for object part segmentation.

2. Related Work

MLP-Based Approaches: PointNet [28] is a milestone in deep learning for point clouds. It employs shared MLPs to leverage point-wise features and a symmetric function such as max-pooling to aggregate these features into global representations. However, the network struggles to exploit local features. To address this issue, hierarchical architectures have been proposed to aggregate local features with MLPs [20, 29] such that the model can benefit from efficient sampling and grouping of the point set. Recent works have focused on enhancing point-wise features by hand-crafting geometric connections [8, 24, 33] or graphs [11, 51, 55]. These MLP-based approaches are simple and effective with fewer learnable parameters.

Convolution-Based Approaches: To improve local feature learning, various point convolutions [40, 41, 44], inspired by 2D grid convolution, dynamically learn convolutional weights (i.e. dynamic kernels) through weight functions from local point geometric connections. KCNet [35], KPConv [37] and KPConvX [38] predefine a set of fixed kernels (coined kernel points) in the local receptive field and then learn the weights on these kernels from the geometric connections between local points and kernel points using Gaussian and linear correlation functions, respectively. Another technique [19, 44] associates coefficients with kernels to further adjust the learned weights, where the coefficients are also derived from point coordinates. Point convolution learns the convolution weights from the low-level point coordinates, lacking high-level semantic awareness. Point convolution methods excel at capturing local features in the initial layers but fail to capture the global context.

Transformer-Based Approaches: To improve semantic awareness and global context learning, point transformers learn attention weights from the feature relationships (i.e., the connections between the query and key) and position differences (i.e., point position encoding). For example, Point Transformer [56] introduces the local vector attention function, to the local points, which learns the weights from the feature differences masked by position encoding. Point Transformer V2 [46], makes the position encoding more complex by introducing a position encoding multiplier to adjust the features. Similarly, the Full Point Transformer [13] operates the position encoding over the global and local receptive fields alternatively, enabling more complex positional encoding. Compared to MLPs and point convolutions, point transformers capture semantic information more effectively. Although local point aggregation methods like MLP, Point Convolution, and Transformer exhibit strong learning capabilities in clean point clouds, they encounter difficulty extracting robust features from noisy point clouds due to their lack of explicit denoising ability.

Diffusion Based Approaches: Diffusion models [14, 27] belong to a class of generative models grounded in Markov

chains that gradually recover data samples through a denoising process. These models have been successful in many generative tasks, spanning image [10, 34] and point cloud generation [25, 39]. Beyond their achievements in generative tasks, diffusion models hold substantial promise for perception tasks such as natural image segmentation [23, 49], medical image segmentation [42, 43] and point part segmentation [48]. Recent works [22, 57] generate points from noisy point clouds to help the backbone capture geometric priors for semantic segmentation. In contrast, our method directly generates *point labels* from noise for semantic segmentation. In this paper, we integrate local point aggregation techniques into the diffusion model and introduce several novel local aggregation modules with denoising capabilities. Building upon our novel local point aggregation techniques, we develop a diffusion model-based semantic segmentation network for large-scale point clouds.

3. Method

We consider a labeled point cloud $\{I_i, x_i^0\} \in \mathbb{R}^{N \times (3+M)}$, where $I_i \in \mathbb{R}^{N \times 3}$ is the point position, $x_i^0 \in \mathbb{R}^{N \times M}$ is the point label, expressed in one-hot form. Here, N is the number of points and M is the number of classes. The corresponding features for point I_i are denoted as F_i . Similar to other diffusion models such as [14], PointDiffuse consists of two stages: a forward diffusion and a reverse diffusion. In the forward diffusion stage, Gaussian noise ϵ is gradually added to the point label x_i^0 as,

$$q(x_i^{1:T} | x_i^0) = \prod_{t=1}^T q(x_i^t | x_i^{t-1}), \quad (1)$$

$$q(x_i^t | x_i^{t-1}) = \mathcal{N}(x_i^t; \sqrt{1 - \beta_t} x_i^{t-1}, \beta_t I_i).$$

The forward process starts with the original point labels x_i^0 and progressively adds noise to it in T steps, generating noisy point labels x_i^T . Therefore, x_i^{t-1} and x_i^t are the noisy point labels at step t and $t - 1$, respectively, in the forward process. $q(x_i^t | x_i^{t-1})$ is a Gaussian transition kernel, which adds noise to the point label input x_i^{t-1} with a variance schedule β_1, \dots, β_T .

During reverse diffusion, a denoising model θ is learned to recover the original point labels from noisy point labels by reversing the noise addition process. This reverse process can be represented as,

$$p_\theta(x_i^{0:T} | x_i^0) = p(x_i^T) \prod_{t=1}^T p_\theta(x_i^{t-1} | x_i^t), \quad (2)$$

$$p_\theta(x_i^{t-1} | x_i^t; S_i, P_{ij}) = \mathcal{N}(x_i^{t-1}; \mu_\theta, \rho_\theta^2 I_i).$$

The reverse process is also Markovian with Gaussian transition kernels, which use fixed variances ρ_θ^2 . Here, S_i represents the additional semantic condition, while P_{ij} denotes the supplementary local position condition, with j in-

dicating the neighborhood point index of point I_i . The reverse process starts from noisy point labels x_i^T and gradually denoises them to recover the original point labels x_i^0 . Therefore, x_i^t and x_i^{t-1} represent the generated point labels at step t and $t - 1$, respectively, in the reverse process. The diffusion model is trained to reverse the forward process, ultimately generating the point label.

$$x_i^{t-1} = \frac{1}{\sqrt{\alpha_t}} \left(x_i^t - \frac{\beta_t}{\sqrt{1 - \bar{\alpha}_t}} \epsilon_\theta(x_i^t, S_i, P_{ij}, t) \right) + \sqrt{\beta_t} \epsilon, \quad (3)$$

where $\alpha_t = 1 - \beta_t$, and $\bar{\alpha}_t = \prod_{s=0}^T \alpha_s$, while ϵ_θ is the noise prediction network, implemented by a learnable network with the parameter set θ . Our diffusion model learns to match generated label x_i^{t-1} with ground truth label x_i^0 by minimizing the difference between ground truth Gaussian noise ϵ and predicted noise $\epsilon_\theta(x_i^t, S_i, P_{ij}, t)$.

3.1. Overall Architecture

To further clarify the PointDiffuse network, we first introduce the single step t of the diffusion process where we define the learnable network ϵ_θ over the input x_i^t and conditions (i.e., semantic and position condition). The learnable *Denoising Network* is expressed as,

$$\epsilon_\theta(x_i^t, S_i, P_{ij}, t) = \text{DNet}_\theta(x_i^t, S_i, P_{ij}, t). \quad (4)$$

Denoising Network DNet_θ is conditioned by the prior information, including semantic information S_i and local position information P_{ij} . The prior information is learned by the *Conditional Network*, which can be expressed as,

$$S_i, P_{ij} = \text{CNet}_\theta(I_i, F_i). \quad (5)$$

Figure 1 shows the overall architecture of PointDiffuse. (a) The noise prediction network in PointDiffuse contains two sub-networks: a conditional network and a denoising network. The conditional network CNet_θ provides the semantic and local position conditions for the denoising network DNet_θ , where the semantic condition refers to the semantic information learned by the conditional network, pre-trained for semantic segmentation. In practice, the conditional network employs a U-Net structure. In our experiments, we employ the state-of-the-art Full Point Transformer network [13] for this. Similarly, the denoising network also adopts a U-Net structure, comprising one noisy label embedding layer, four encoding layers, four decoding layers, and one noise prediction head. Each of the first three encoding layers contains a Shared Transition Down and a Denoising PointNet, while the last encoding layer contains a Shared Transition Down and a Point Frequency Transformer. Each of the last three decoding layers contains a Shared Transition Up and a Denoising PointNet, while the first decoding layer contains a Shared Transition Up and a Point Frequency Transformer. The Shared Transition Down/Up denotes that Transition Down/Up blocks [56] with the same encoding/decoding

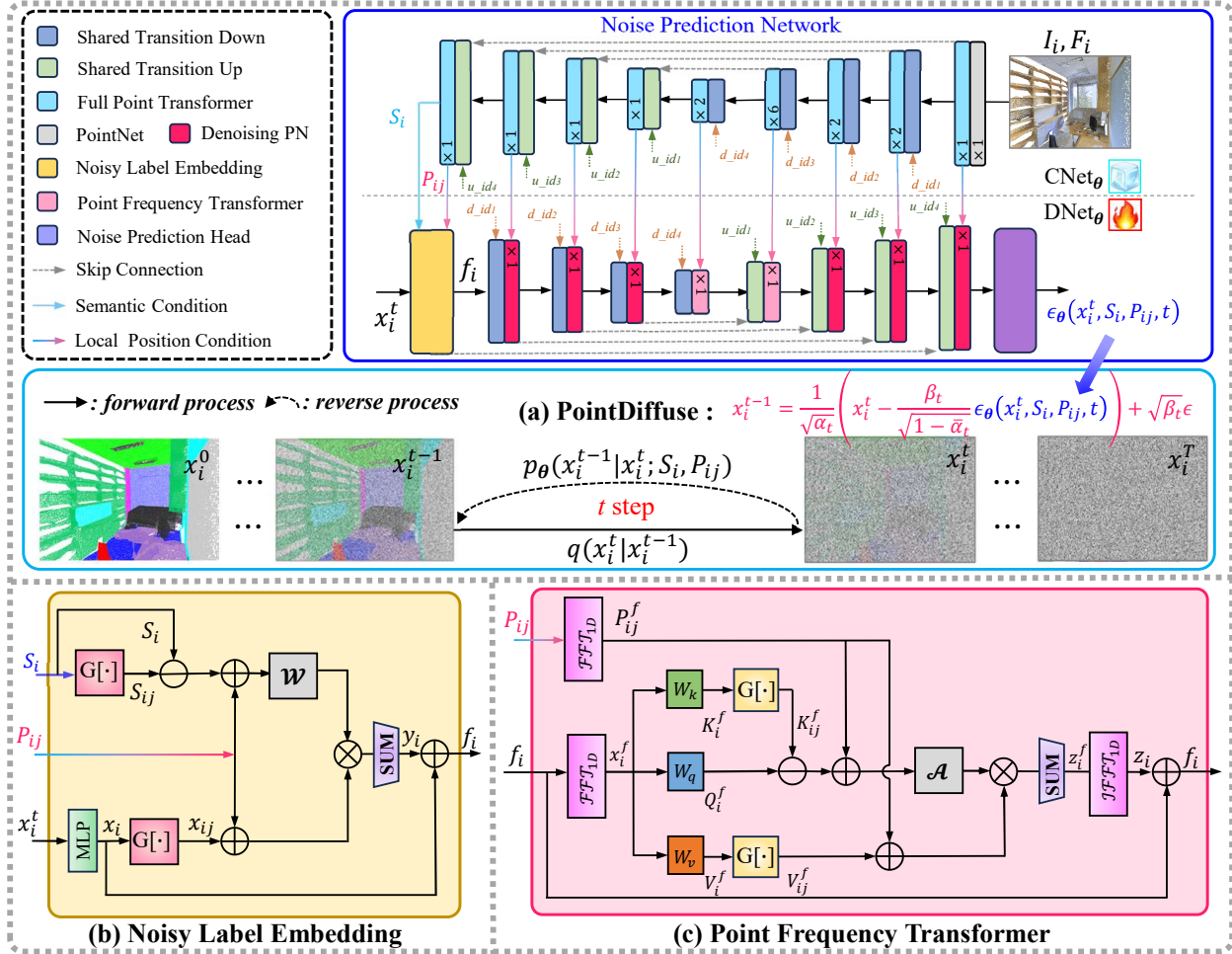


Figure 1. An illustration of PointDiffuse, starting with (a) an overview of the entire pipeline, followed by detailed views of its key sub-modules: (b) Noisy Label Embedding for variance stabilization and (c) Point Frequency Transformer for noise filtering.

layer share identical neighborhood point indexes across the same resolution points.

During training, we freeze the parameters of the pre-trained conditional network and train the denoising network. This training, at each step in the reverse process, uses a standard noise prediction loss \mathcal{L}_n^t along with a label generation cross-entropy loss \mathcal{L}_{ce} . The total loss becomes:

$$\begin{aligned} \mathcal{L}_{total} &= \gamma \mathcal{L}_n^t + (1 - \gamma) \mathcal{L}_{ce} \\ &= \gamma \| \epsilon - \epsilon_\theta(x_i^t, S_i, P_{ij}, t) \|^2 + (1 - \gamma) \| x_i^0 - x_i^{t-1} \|^2, \end{aligned} \quad (6)$$

where $\epsilon \sim \mathcal{N}(0, I_i)$ and $\gamma \in (0, 1)$ is a hyperparameter that balances the contribution of the loss terms.

3.2. Noisy Label Embedding

High variance at each denoising step can lead to instability, requiring more diffusion steps to achieve the desired outcome, which ultimately results in suboptimal model performance. To overcome this, we propose a novel noisy label

embedding module that leverages semantic and position information to condition the noisy label embedding, stabilizing the variance during diffusion. As shown in Figure 1 (b), the noisy label embedding on each point can be expressed as,

$$\begin{aligned} x_i &= \text{MLP}(x_i^t), \\ y_i &= \sum_{j=1}^K \mathcal{W}((G[S_i] \ominus S_i) \oplus P_{ij}) \otimes (G[x_i] \oplus P_{ij}), \\ &= \sum_{j=1}^K \mathcal{W}((S_{ij} \ominus S_i) \oplus P_{ij}) \otimes (x_{ij} \oplus P_{ij}), \\ f_i &= y_i \oplus x_i, \end{aligned} \quad (7)$$

where the summation aggregates the features over K neighborhood points. $G[\cdot]$ is the grouping operation to group the global element (i.e., S_i or x_i) into the local receptive field, yielding the local elements (i.e., S_{ij} or x_{ij}). \ominus, \otimes, \oplus are

the element-wise subtraction, multiplication, and addition operations, respectively.

During noisy label embedding, we first use an MLP to project the noisy labels x_i^t onto noisy features x_i . Next, we integrate the semantic S_i and local position condition P_{ij} into noisy features to obtain enhanced noisy features y_i . In particular, we construct local semantic connections, incorporate local position information, and then learn the weights using a weight function $\mathcal{W}(\cdot)$ from these connections to adjust the noisy features. Finally, we add the enhanced noisy feature y_i to the original noisy features x_i to obtain the noisy label embedding f_i , retaining important information that could potentially be lost.

Compared to classic point convolution, the proposed noisy label embedding offers two key advantages: **i)** Noisy label embedding learns the weights from the semantic conditions rather than simple coordination differences. Semantic conditions, derived from the final layer of the condition network, provide a rough but stable semantic reference for noisy features, significantly reducing the diffusion variance. In addition, this allows the semantic features to be further refined during denoising. **ii)** Inspired by the position encoding in the point transformer, we equip the semantic connection with the local position condition to be better aware of the point cloud structure and further restrain the geometry detail loss. This not only reduces the number of network training parameters but also ensures that both conditional and denoising networks perceive the same point positions. Such an alignment also helps prevent instability and performance degradation from inconsistent position encoding.

3.3. Point Frequency Transformer

The denoising network predicts the noise component from the noisy labels. While conventional point transformers effectively embed features, they struggle to learn noise in the spatial domain [52]. Motivated by this problem, we propose a novel point frequency transformer that operates in the frequency domain given the noisy input feature $f_i \in \mathbb{R}^{N \times C}$ and the local position condition $P_{ij} \in \mathbb{R}^{N \times K \times C}$.

Figure 1 (c) shows our Point Frequency Transformer. First, we separately perform 1-D Fast Fourier Transform ($\mathcal{F}\mathcal{F}\mathcal{T}_{1D}$) on the noisy features f_i along the N dimension and on the local position condition P_{ij} along the K dimension. The transformed noisy features x_i^f and local position conditions P_{ij}^f in the frequency domain are represented as,

$$x_i^f = \mathcal{F}\mathcal{F}\mathcal{T}_{1D}(f_i), \quad P_{ij}^f = \mathcal{F}\mathcal{F}\mathcal{T}_{1D}(P_{ij}). \quad (8)$$

We then learn the query Q_i^f , key K_i^f , value V_i^f from these transformed noisy features,

$$Q_i^f = W_q(x_i^f), \quad K_i^f = W_k(x_i^f), \quad V_i^f = W_v(x_i^f), \quad (9)$$

where W_q, W_k, W_v are the project functions. The point frequency transformer is,

$$\begin{aligned} z_i^f &= \sum_{j=1}^K \mathcal{A}((G[K_i^f] \ominus Q_i^f) \oplus P_{ij}^f) \otimes (G[V_i^f] \oplus P_{ij}^f), \\ &= \sum_{j=1}^K \mathcal{A}((K_{ij}^f \ominus Q_i^f) \oplus P_{ij}^f) \otimes (V_{ij}^f \oplus P_{ij}^f), \end{aligned} \quad (10)$$

where $\mathcal{A}(\cdot)$ is the attention weight function, implemented by an MLP followed by a softmax. We project the feature learned by the transformer from the frequency domain back to the spatial domain by a 1-D Inverse Fast Fourier Transform ($\mathcal{I}\mathcal{F}\mathcal{F}\mathcal{T}_{1D}$). Finally, we use a residual connection from f_i to avoid missing useful information.

$$\begin{aligned} z_i &= \mathcal{I}\mathcal{F}\mathcal{F}\mathcal{T}_{1D}(z_i^f), \\ f_i &= z_i \oplus f_i. \end{aligned} \quad (11)$$

By mapping features to the frequency domain, the point frequency transformer can separate low-frequency components, which represent the underlying structure, from high-frequency components, which are often associated with noise. This separation enables the model to more effectively distinguish between critical features and noise, thus improving segmentation performance. Furthermore, by masking the grouped global noise with local noise positions, the point frequency transformer can more effectively identify local noise, improving its local denoising capability.

3.4. Denoising PointNet

The complex Point Frequency Transformer applied to high-resolution point clouds incurs a significant computational burden leading to long runtime. To alleviate this problem, we propose a simple and efficient Denoising PointNet over the high resolution point cloud. It can be expressed as,

$$\begin{aligned} f_i &= \Lambda_{j=1}^K \text{MLP}(G[f_i] \oplus P_{ij}) \\ &= \Lambda_{j=1}^K \text{MLP}(f_{ij} \oplus P_{ij}) \end{aligned} \quad (12)$$

where $\Lambda_{j=1}^K$ is the maxpooling operation over K neighborhood points. Incorporating the local position condition into the noisy features before applying MLP helps preserve spatial information and reduces the MLP's sensitivity to noise. This enhances the model's generalization and adaptability, while also reducing runtime compared to more complex local denoising aggregation methods.

4. Experiments

4.1. Evaluation Setup

Datasets. We conduct experiments on five popular datasets: S3DIS, ScanNetv2, SWAN, SemanticKITTI and ShapeNet. S3DIS [1] includes colored point clouds of 6 large-scale indoor scenes. Our evaluation employs Area 5 and 6-fold cross-validation on these 6 indoor scenes. ScanNet [7] contains colored point clouds of indoor scenes. It is split into

Year	Methods	S3DIS 6-fold			Area 5		Scan.	S.KI	SW.	Shape.
		mIoU	Para. FLOPs		mIoU	mIoU	mIoU	mIoU	Ins. mIoU	
<i>previous state-of-the-art point convolution based methods</i>										
ICCV'19	KPCConv[37]	70.6	15	-	67.1	69.2	-	-	-	86.4
CVPR'21	PACConv [50]	69.3	-	-	66.6	-	-	-	-	86.1
CVPR'24	KPCConvX [38]	-	13.5	-	73.5	76.3	-	-	-	-
<i>previous state-of-the-art MLP-based methods</i>										
NIPS'22	PointNeXt [30]	74.9	41.6	84.8	71.1	71.5	-	50.4	-	87.2
CVPR'23	PointVector [8]	78.4	24.1	58.5	72.3	-	-	-	-	86.9
CVPR'23	PointMeta [21]	77.0	19.7	11.0	71.3	72.8	-	-	-	87.1
<i>previous state-of-the-art point transformer based methods</i>										
ICCV'21	PT [56]	73.5	7.8	5.6	70.4	70.4	-	58.6	-	86.6
CVPR'22	ST [18]	-	-	-	72.0	74.3	-	-	-	86.6
NIPS'22	PT V2 [46]	75.2	12.8	-	71.6	75.4	70.3	59.7	-	-
NIPS'23	ConDAF [9]	-	-	-	<u>73.5</u>	76.0	-	-	-	-
CVPR'24	PT V3 [47]	77.7	42.6	-	73.1	77.5	70.8	61.1	-	-
TNNLS'24	FPT [13]	76.8	10.9	8.3	73.1	75.6	69.6	<u>61.8</u>	-	87.1
<i>diffusion based method</i>										
ICCV'23	STPD [48]	-	-	-	-	-	-	-	-	86.7
CASSP'24	Liu et al [22]	<u>80.8</u>	-	-	-	-	-	-	-	89.3
ArXiv'24	CDSegNet [32]	-	-	-	-	<u>77.9</u>	-	-	-	-
CVPR'24	PointDif [57]	-	-	-	70.0	-	<u>71.3</u>	-	-	-
	PointDiffuse	81.2	15.2	7.3	74.2	78.2	71.4	64.8	-	<u>88.4</u>

Table 1. Segmentation results on 5 datasets. We report mIoU for S3DIS (6-fold and Area 5), ScanNet, SemanticKITTI and SWAN datasets. For part segmentation on ShapeNet, we report Ins. mIoU. We also report Parameters (million) and FLOPs (giga) for S3DIS dataset. In each column, the best result is bolded and second best is underlined. % signs are omitted for clarity. Scan. = ScanNet; S.KI = SemanticKITTI; SW. = SWAN; Shape. = ShapeNet. All methods do not use the multi-dataset for joint training.

1,201 scenes for training and 312 scenes for validation. SemanticKITTI [3] is an outdoor dataset using sequences 0 to 10 (excluding 8) for training and sequence 8 for validation. SWAN [17] is a more recent outdoor dataset, where sequences 0 to 23 are allocated for training and sequences 24 to 31 are designated for testing. ShapeNet [53] is a 3D object part segmentation dataset, where 14,006 objects are used for training and 2,874 for testing.

Data Pre-processing. We follow data pre-processing strategies similar to previous methods[13, 47, 56]. For example, we subsample the input point cloud using the 4cm grid for S3DIS and set the maximum number of subsampled points to 80,000. We adopt random scaling, random flipping, chromatic contrast, chromatic translation, and chromatic jitter to augment training data. More details are in *Supplementary Material*.

Implementation Details. All experiments are conducted on the PyTorch platform and trained/tested on 4 NVIDIA 3090 GPUs. On the indoor S3DIS dataset, we pre-train the conditional network, gathering point labels from the training set of a single dataset due to limited computational resources without using multi-dataset joint training. The de-

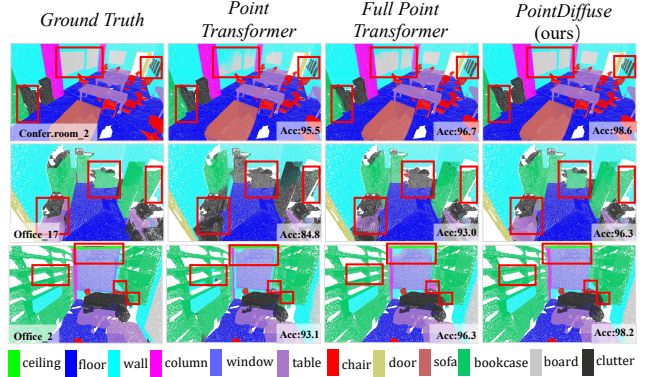


Figure 2. Semantic segmentation results on S3DIS Area-5. Red boxes indicate areas where our proposed PointDiffuse demonstrates noticeable improvements over previous methods, such as Point Transformer and Full Point Transformer.

noising network is trained in an end-to-end manner using the AdamW optimizer with a batch size of 12. The initial learning rate is set to 0.5 and adjusted using MultiStepLR. Details are in *Supplementary Material*.

Evaluation Metrics. We report three evaluation metrics including mIoU, parameters and FLOPs for S3DIS Area 5 experiment. On S3DIS 6-fold, ScanNet, SemanticKITTI and SWAN dataset, we report the mIoU metric and on ShapeNet, we report the Ins. mIoU metric.

4.2. Comparison with State-of-the-art Methods

To verify the general point cloud segmentation performance, we compare PointDiffuse with recent state-of-the-art methods on five datasets without using multi-dataset joint training. Results are compiled in Table 1.

On the S3DIS indoor dataset 6-fold validation, our method achieves a state-of-the-art performance of 81.2% mIoU, surpassing the diffusion-based method [22] by 0.4% mIoU. Our method outperforms Point Transformer [56] (including V2 [46] and V3 [47]) and Full Point Transformer [13] by large margins. On the S3DIS Area 5, our method also achieves the best performance of 74.2% mIoU, outperforming the diffusion-based method (i.e., PointDif [57]) by **4.2% mIoU**. Furthermore, it exceeds the previous state-of-the-art MLP-based approach (i.e., PointVector [8]) by **1.9% mIoU**, while using only **63.1% parameters** and **12.5% FLOPs**. Visualizations of our results on Area 5 are shown in Figure 2.

On the ScanNet indoor dataset, our method achieves the best result (i.e., 78.2% mIoU) on the validation set, outperforming the diffusion-based method CDSegNet [32].

On the SemanticKITTI outdoor dataset, our method achieves 71.4% mIoU on the validation set, outperforming transformer-based methods (e.g., Point Transformer V3 and Full Point Transformer) and diffusion-based method (i.e., PointDif [57]).

Case	D-PN	NLE/ <i>w</i> SC	NLE/ <i>w</i> PC	PFT	S3DIS(%)	S.KITTI(%)
I	✓				71.6	67.4
II	✓	✓			73.2	69.6
III	✓	✓	✓		73.7	70.6
IV	✓	✓	✓	✓	74.2	71.4
V	✓	✓		✓	73.8	70.9
VI	✓		✓	✓	72.4	70.4

Table 2. Effect of various components. D-PN: Denoising PointNet. NLE = Noisy Label Embedding. *w* SC = with semantic condition. *w* PC = with position condition. PFT = Point Frequency Transformer. Metric: mIoU.

Backbone	PT	PT V2	FPT
step 5	68.4	71.9	72.4
step 10	70.5	74.3	75.0
step 15	72.4	76.3	78.0
step 20	72.5	76.4	78.2
step 25	72.5	76.4	78.3
step 30	72.5	76.4	78.4

Table 3. Semantic segmentation on ScanNet. PT = Point Transformer. PT V2 = Point Transformer V2. FPT = Full Point Transformer. Metric: mIoU(%).

On the *SWAN* outdoor dataset, we compare our results to the convolution-based method PointConv [44], MLP-based method PointNext [30], and transformer-based methods Point Transformer (including V2 and V3) and Full Point Transformer. These results are obtained by carefully training the models using the author-provided code and guidelines. Our PointDiffuse gets the best performance at 64.8% mIoU, exceeding the nearest competitor, Point Transformer V3 [47], by **3%**.

On the *ShapeNet* object dataset, our method achieves a competitive performance of 88.4% Ins. mIoU, compared to traditional deep learning models. Notably, our method outperforms the previous diffusion-based method STPD [48] by 1.7%.

Our results show that the proposed PointDiffuse outperforms all existing diffusion-based methods on the scene segmentation task but is only slightly worse than the method proposed by Liu et al. [22] in the part segmentation task. This is potentially because scene point clouds contain more noise compared to object point clouds. Since our method directly denoises labels, it is particularly effective in generating accurate labels for noisy scene point clouds.

4.3. Ablation Study

We perform ablation experiments on the S3DIS and SemanticKITTI datasets to verify the effectiveness of the Denoising PointNet, Noisy Label Embedding, and Point Frequency Transformer in the PointDiffuse network. Additional ablation studies are in *Supplementary Material*.

Effect of Various Components. The effect of various components of PointDiffuse are shown in Table 2. **i)** Case I is the baseline simple PointDiffuse. Its denoising predic-

γ	0.3	0.4	0.5	0.6	0.7
S3DIS(%)	72.4	73.0	74.2	72.4	71.4
S.KITTI(%)	69.3	70.2	71.0	71.4	70.8

Table 4. Effect of hyper-parameter γ on performance.

Case	I		II		III	
	mIoU	Time/s	mIoU	Time/s	mIoU	Time/s
step 5	69.0	195	68.8	109	68.5	49
step 10	71	390	70.9	218	70.6	98
step 15	73.8	585	73.0	327	72.6	147
step 20	74.6	780	74.4	436	74.2	196
step 25	74.6	975	74.4	545	74.2	245
step 30	74.6	1170	74.4	654	74.3	294

Table 5. Segmentation accuracy and time (in sec) per scene on S3DIS Area 5 with different number of Denoising PointNet. *s* = second.

tion network consists of the conditional network Full Point Transformer [13] and simplified PointNet++. The set abstraction module in the PointNet++ is replaced with the proposed Denoising PointNet. **ii)** Cases II to IV systematically incorporate each of our proposed components, progressively enhancing the baseline results to reach 74.2% and 71.4% on the S3DIS Area 5 and SemanticKITTI validation set, respectively. **iii)** In Case V and VI, we remove the semantic and positions conditions from the noisy label embedding. Results indicate that the semantic condition is more crucial than the position condition.

Effect of Conditional Network Backbone. We study the impact of different backbones for the conditional network using Point Transformer [56], Point Transformer V2 [46], or Full Point Transformer [13] in Table 3. PointDiffuse model with all three types of backbones achieve stable performance at step 20. However, using Full Point Transformer for the conditional network achieves the highest performance, with an accuracy of 78.4% mIoU. Hence, we select the Full Point Transformer as the backbone of conditional network, and adopt 20 diffusion steps to balance both accuracy and training efficiency for the ScanNet dataset.

Effect of Loss. We vary the hyper-parameter γ in equation 6 and observe the performance of our network on S3DIS and SemanticKITTI. Table 4 shows that the best performance is achieved with 0.5 and 0.6, respectively.

4.4. Further Analysis

Runtime Analysis. Table 5 shows results for our runtime analysis. The number and position of Denoising PointNet layers in the denoising network significantly influence training efficiency. The case I/II/III denotes the Denoising PointNet with the first one/two/three encoding layers and the last one/two/three decoding layers. Specifically, Case III, which places Denoising PointNet in the first three encoding layers and the last three decoding layers, achieves the shortest runtime—approximately 10 seconds per step.

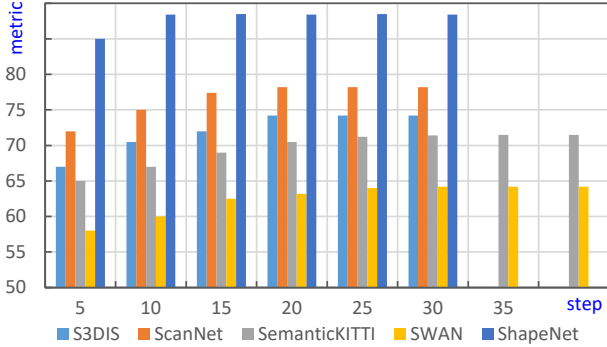


Figure 3. The effect of sampling step of PointDiffuse. We show the performance of metric (mIoU or Ins.mIoU) with increasing sampling steps.

Method	mIoU	mAcc	OA	Paras.(M)	FLOPs(G)
PointNet [28]	47.6	66.2	78.5	3.6	35.5
PointNet++ [29]	54.5	67.1	81.0	1	7.2
RandLA-Net [16]	70.0	82.0	88.0	1.3	5.8
Point Transformer [56]	73.5	81.9	90.2	7.8	5.6
PointNext-XL [30]	74.9	83.0	90.3	41.6	84.8
PointVector-XL [8]	78.4	86.1	91.9	24.1	58.5
PointDiffuse/wt STD/U	79.4	87.3	92.4	15.2	10.9
PointDiffuse/w STD/U	79.4	87.3	92.4	15.2	7.3

Table 6. Semantic segmentation on S3DIS with 6-fold validation

Sampling Step Analysis. We study the impact of different sampling steps for point cloud segmentation on indoor, outdoor, and object datasets (see Figure 3). Depending on their complexity, different datasets require different numbers of sampling steps. We adopt 20, 30, and 15 steps for indoor, outdoor, and object datasets for optimal performance. We can observe that our network achieves the best performance with a few sampling steps on all datasets. Note that outdoor datasets require more steps than indoor datasets, and the object dataset requires the least steps. There are two potential reasons for this: **i)** Outdoor scenes contain a larger number of multi-scale objects and complex geometric structures, requiring more diffusion steps to gradually disentangle semantic-geometric relationships. **ii)** Noise in indoor datasets is closer to the standard Gaussian assumption, facilitating faster convergence.

Analysis on Shared Transition Down/Up. We conduct a comparative analysis between a noise prediction network employing shared Transition Down/Up and another utilizing Transition Down/Up while maintaining consistency in the remaining network configuration. Our results in Table 6 highlight the advantage of the Shared Transition Down/Up block as it achieves a similar performance to the one with Transition Down/Up block but with 33% fewer FLOPs (7.3G vs 10.9G FLOPs). Note that the accuracy and number of parameters remain unchanged because the shared down-sampling mechanism only shares neighborhood point indices to avoid redundant computations, without altering the learnable parameters of the network.

Methods	None	Perm.	Rotation			Shifting		Scaling		Jitter
			$\pi/2$	π	$3\pi/2$	+0.2	-0.2	$\times 0.8$	$\times 1.2$	
PointNet++	59.75	59.71	58.15	57.18	58.19	22.33	29.85	56.24	59.74	59.04
Minkowski	64.68	64.56	63.45	63.83	63.36	64.59	64.96	59.60	61.93	58.96
PAConv	65.63	65.64	61.66	63.48	61.80	55.81	57.42	64.20	63.94	65.12
Point Tr.	70.36	70.45	65.94	67.78	65.72	70.44	70.43	65.73	66.15	59.67
S.Tr.	71.96	72.02	72.59	72.37	71.86	71.99	71.93	70.42	71.21	72.02
PointVe.	72.29	-	72.27	72.30	72.32	72.29	72.29	69.34	69.26	72.16
FPtr.	72.21	72.23	-	-	-	72.31	72.42	72.09	71.48	72.31
Ours	73.36	73.35	73.76	72.94	73.26	73.47	73.46	72.54	73.10	73.38

Table 7. Robustness study on S3DIS (mIoU%) for random point permutations, Z axis rotation ($\pi/2$, π , $3\pi/2$), shifting (± 0.2), scaling ($\times 0.8, \times 1.2$) and jitter in testing. Point Tr. = Point Transformer. S.Tr. = Stratified Transformer. PointVe. = PointVector. FPtr. = Full Point Transformer.

Analysis on Perturbation Robustness. In Table 7, we evaluate the robustness of our model to perturbations during testing. Following [50], we apply perturbations such as permutation, rotation, shifting, scaling, and jitter to the point clouds. **i)** Our method achieves the best performance of 73.46% mIoU without traditional data augmentation, demonstrating that the gains come from the diffusion model itself rather than the augmentation process. **ii)** our method is extremely robust to various perturbations. This further indicates that the diffusion model’s ability to improve robustness comes from its denoising property. By removing Gaussian noise (which represents random perturbations), the diffusion model helps the model focus on the underlying data distribution rather than specific perturbation details. This denoising process trains the model to learn more robust features that are less sensitive to variations such as rotation, scaling, and jitter, thus improving performance under these perturbations.

5. Conclusion and Limitation

We proposed a novel dual conditional diffusion model-based network for point cloud semantic segmentation. To stabilize variance in the diffusion process, we introduced a Noisy Label Embedding mechanism, integrating both semantic and local position conditions. Furthermore, we designed a Point Frequency Transformer to effectively filter local geometric and global context noise. We developed a simple yet effective Denoising PointNet, which significantly reduces runtime. Extensive experiments across diverse datasets validate the robustness and efficacy of our approach.

Limitation: Due to resource constraints, we have not yet been able to utilize multiple datasets for joint training of the conditional network. We believe that doing so could further enrich the learned representations and enhance the segmentation performance.

6. Acknowledgment

This work was supported by National Key R&D Program (2023YFB4704500), National Natural Science Foundation of China under Grant (U2013203, 62373140, U21A20487, 62103137), the Project of Science Fund for Distinguished Young Scholars of Hunan Province (2021JJ10024); Leading Talents in Science and Technology Innovation of Hunan Province (2023RC1040), the Project of Science Fund of Hunan Province (2022JJ30024); the Project of Talent Innovation and Sharing Alliance of Quanzhou City (2021C062L); the Key Research and Development Project of Science and Technology Plan of Hunan Province (2022GK2014). Professor Ajmal Mian is the recipient of an Australian Research Council Future Fellowship Award (project number FT210100268) funded by the Australian Government.

References

- [1] Iro Armeni, Ozan Sener, Amir R Zamir, Helen Jiang, Ioannis Brilakis, Martin Fischer, and Silvio Savarese. 3d semantic parsing of large-scale indoor spaces. In *Proceedings of the IEEE/CVF Conference on Computer Vision and Pattern Recognition*, pages 1534–1543, 2016. 2, 5
- [2] Arpit Bansal, Hong-Min Chu, Avi Schwarzschild, Soumyadip Sengupta, Micah Goldblum, Jonas Geiping, and Tom Goldstein. Universal guidance for diffusion models. In *Proceedings of the IEEE/CVF Conference on Computer Vision and Pattern Recognition*, pages 843–852, 2023. 1
- [3] Jens Behley, Martin Garbade, Andres Milioto, Jan Quenzel, Sven Behnke, Cyrill Stachniss, and Jurgen Gall. Semantickitti: A dataset for semantic scene understanding of lidar sequences. In *Proceedings of the IEEE International Conference on Computer Vision*, pages 9297–9307, 2019. 2, 6
- [4] Shoufa Chen, Peize Sun, Yibing Song, and Ping Luo. Diffusiondet: Diffusion model for object detection. In *Proceedings of the IEEE/CVF International Conference on Computer Vision*, pages 19830–19843, 2023. 1
- [5] Yen-Chi Cheng, Hsin-Ying Lee, Sergey Tulyakov, Alexander G Schwing, and Liang-Yan Gui. Sdfusion: Multimodal 3d shape completion, reconstruction, and generation. In *Proceedings of the IEEE/CVF Conference on Computer Vision and Pattern Recognition*, pages 4456–4465, 2023. 1
- [6] Sammy Christen, Wei Yang, Claudia Pérez-D’Arpino, Otmar Hilliges, Dieter Fox, and Yu-Wei Chao. Learning human-to-robot handovers from point clouds. In *Proceedings of the IEEE/CVF Conference on Computer Vision and Pattern Recognition*, pages 9654–9664, 2023. 1
- [7] Angela Dai, Angel X Chang, Manolis Savva, Maciej Halber, Thomas Funkhouser, and Matthias Nießner. Scannet: Richly-annotated 3d reconstructions of indoor scenes. In *Proceedings of the IEEE/CVF Conference on Computer Vision and Pattern Recognition*, pages 5828–5839, 2017. 2, 5
- [8] Xin Deng, WenYu Zhang, Qing Ding, and XinMing Zhang. Pointvector: A vector representation in point cloud analysis. In *Proceedings of the IEEE/CVF Conference on Computer Vision and Pattern Recognition*, pages 9455–9465, 2023. 1, 2, 6, 8
- [9] Lunhao Duan, Shanshan Zhao, Nan Xue, Mingming Gong, Gui-Song Xia, and Dacheng Tao. Condaformer: Disassembled transformer with local structure enhancement for 3d point cloud understanding. *Advances in Neural Information Processing Systems*, 36, 2024. 6
- [10] Dave Epstein, Allan Jabri, Ben Poole, Alexei Efros, and Aleksander Holynski. Diffusion self-guidance for controllable image generation. *Advances in Neural Information Processing Systems*, 36:16222–16239, 2023. 3
- [11] Mingtao Feng, Liang Zhang, Xuefei Lin, Syed Zulqarnain Gilani, and Ajmal Mian. Point attention network for semantic segmentation of 3d point clouds. *Pattern Recognit.*, 107: 107446, 2020. 2
- [12] Yong He, Hongshan Yu, Zhengeng Yang, Wei Sun, Mingtao Feng, and Ajmal Mian. Danet: Density adaptive convolutional network with interactive attention for 3d point clouds. *IEEE Robotics and Automation Letters*, 2023. 1
- [13] Yong He, Hongshan Yu, Zhengeng Yang, Xiaoyan Liu, Wei Sun, and Ajmal Mian. Full point encoding for local feature aggregation in 3-d point clouds. *IEEE Transactions on Neural Networks and Learning Systems*, pages 1–15, 2024. 1, 2, 3, 6, 7
- [14] Jonathan Ho, Ajay Jain, and Pieter Abbeel. Denoising diffusion probabilistic models. *Advances in Neural Information Processing Systems*, 33:6840–6851, 2020. 1, 2, 3
- [15] Haoran Hou, Mingtao Feng, Zijie Wu, Weisheng Dong, Qing Zhu, Yaonan Wang, and Ajmal Mian. 3d object detection from point cloud via voting step diffusion. *arXiv preprint arXiv:2403.14133*, 2024. 1
- [16] Qingyong Hu, Bo Yang, Linhai Xie, Stefano Rosa, Yulan Guo, Zhihua Wang, Niki Trigoni, and Andrew Markham. Randla-net: Efficient semantic segmentation of large-scale point clouds. In *Proceedings of the IEEE/CVF Conference on Computer Vision and Pattern Recognition*, pages 11108–11117, 2020. 8
- [17] Muhammad Ibrahim, Naveed Akhtar, Saeed Anwar, and Ajmal Mian. Sat3d: Slot attention transformer for 3d point cloud semantic segmentation. *IEEE Trans. Intell. Transp. Syst.*, 2023. 2, 6
- [18] Xin Lai, Jianhui Liu, Li Jiang, Liwei Wang, Hengshuang Zhao, Shu Liu, Xiaojuan Qi, and Jiaya Jia. Stratified transformer for 3d point cloud segmentation. In *Proceedings of the IEEE/CVF Conference on Computer Vision and Pattern Recognition*, pages 8500–8509, 2022. 1, 6
- [19] Huan Lei, Naveed Akhtar, and Ajmal Mian. Seggcn: Efficient 3d point cloud segmentation with fuzzy spherical kernel. In *Proceedings of the IEEE/CVF Conference on Computer Vision and Pattern Recognition*, 2020. 2
- [20] Jiaxin Li, Ben M Chen, and Gim Hee Lee. So-net: Self-organizing network for point cloud analysis. In *Proceedings of the IEEE/CVF Conference on Computer Vision and Pattern Recognition*, pages 9397–9406, 2018. 2

- [21] Haojia Lin, Xiawu Zheng, Lijiang Li, Fei Chao, Shanshan Wang, Yan Wang, Yonghong Tian, and Rongrong Ji. Meta architecture for point cloud analysis. In *Proceedings of the IEEE/CVF Conference on Computer Vision and Pattern Recognition*, pages 17682–17691, 2023. 1, 6
- [22] Chang Liu, Aimin Jiang, Yibin Tang, Yanping Zhu, and Qi Chen. 3d point cloud semantic segmentation based on diffusion model. In *ICASSP 2024-2024 IEEE International Conference on Acoustics, Speech and Signal Processing (ICASSP)*, pages 4375–4379. IEEE, 2024. 3, 6, 7
- [23] Daochang Liu, Qiyue Li, Anh-Dung Dinh, Tingting Jiang, Mubarak Shah, and Chang Xu. Diffusion action segmentation. In *Proceedings of the IEEE/CVF International Conference on Computer Vision*, pages 10139–10149, 2023. 3
- [24] Xu Ma, Can Qin, Haoxuan You, Haoxi Ran, and Yun Fu. Rethinking network design and local geometry in point cloud: A simple residual mlp framework. In *Proc. Int. Conf. Learn. Represent.*, 2021. 2
- [25] Vinicius Mikuni, Benjamin Nachman, and Mariel Pettee. Fast point cloud generation with diffusion models in high energy physics. *Physical Review D*, 108(3):036025, 2023. 3
- [26] Shentong Mo, Enze Xie, Ruihang Chu, Lanqing Hong, Matthias Niessner, and Zhenguo Li. Dit-3d: Exploring plain diffusion transformers for 3d shape generation. *Advances in Neural Information Processing Systems*, 36, 2024. 1
- [27] Alexander Quinn Nichol and Prafulla Dhariwal. Improved denoising diffusion probabilistic models. In *International conference on machine learning*, pages 8162–8171. PMLR, 2021. 2
- [28] Charles R Qi, Hao Su, Kaichun Mo, and Leonidas J Guibas. Pointnet: Deep learning on point sets for 3d classification and segmentation. In *Proceedings of the IEEE/CVF Conference on Computer Vision and Pattern Recognition*, pages 652–660, 2017. 2, 8
- [29] Charles R Qi, Li Yi, Hao Su, and Leonidas J Guibas. Pointnet++: Deep hierarchical feature learning on point sets in a metric space. *arXiv preprint arXiv:1706.02413*, 2017. 2, 8
- [30] Guocheng Qian, Yuchen Li, Houwen Peng, Jinjie Mai, Hasan Hammoud, Mohamed Elhoseiny, and Bernard Ghanem. Pointnext: Revisiting pointnet++ with improved training and scaling strategies. In *Advances in Neural Information Processing Systems*, 2022. 1, 6, 7, 8
- [31] Tianwen Qian, Jingjing Chen, Linhai Zhuo, Yang Jiao, and Yu-Gang Jiang. Nuscenes-qa: A multi-modal visual question answering benchmark for autonomous driving scenario. In *Proceedings of the AAAI Conference on Artificial Intelligence*, pages 4542–4550, 2024. 1
- [32] Wentao Qu, Jing Wang, YongShun Gong, Xiaoshui Huang, and Liang Xiao. An end-to-end robust point cloud semantic segmentation network with single-step conditional diffusion models. *arXiv preprint arXiv:2411.16308*, 2024. 6
- [33] Haoxi Ran, Jun Liu, and Chengjie Wang. Surface representation for point clouds. In *Proceedings of the IEEE/CVF Conference on Computer Vision and Pattern Recognition*, 2022. 2
- [34] Robin Rombach, Andreas Blattmann, Dominik Lorenz, Patrick Esser, and Björn Ommer. High-resolution image synthesis with latent diffusion models. In *Proceedings of the IEEE/CVF Conference on Computer Vision and Pattern Recognition*, pages 10684–10695, 2022. 3
- [35] Yiru Shen, Chen Feng, Yaoqing Yang, and Dong Tian. Mining point cloud local structures by kernel correlation and graph pooling. In *Proceedings of the IEEE/CVF Conference on Computer Vision and Pattern Recognition*, pages 4548–4557, 2018. 2
- [36] Nikolaos Stathoulopoulos, Anton Koval, Ali-akbar Aghamohammadi, and George Nikolakopoulos. Frame: Fast and robust autonomous 3d point cloud map-merging for egocentric multi-robot exploration. In *2023 IEEE International Conference on Robotics and Automation*, pages 3483–3489. IEEE, 2023. 1
- [37] Hugues Thomas, Charles R Qi, Jean-Emmanuel Deschaud, Beatriz Marcotequi, François Goulette, and Leonidas J Guibas. Kpconv: Flexible and deformable convolution for point clouds. In *Proceedings of the IEEE International Conference on Computer Vision*, pages 6411–6420, 2019. 2, 6
- [38] Hugues Thomas, Yao-Hung Hubert Tsai, Timothy D Barfoot, and Jian Zhang. Kpconvx: Modernizing kernel convolution with kernel attention. *arXiv preprint arXiv:2405.13194*, 2024. 1, 2, 6
- [39] Michał J Tyszkiewicz, Pascal Fua, and Eduard Trulls. Gecco: Geometrically-conditioned point diffusion models. In *Proceedings of the IEEE/CVF International Conference on Computer Vision*, pages 2128–2138, 2023. 3
- [40] Shenlong Wang, Simon Suo, Wei-Chiu Ma, Andrei Pokrovsky, and Raquel Urtasun. Deep parametric continuous convolutional neural networks. In *Proceedings of the IEEE/CVF Conference on Computer Vision and Pattern Recognition*, pages 2589–2597, 2018. 2
- [41] Yue Wang, Yongbin Sun, Ziwei Liu, Sanjay E Sarma, Michael M Bronstein, and Justin M Solomon. Dynamic graph cnn for learning on point clouds. *ACM Transactions on Graphics*, 38(5):1–12, 2019. 2
- [42] Junde Wu, Rao Fu, Huihui Fang, Yu Zhang, Yehui Yang, Haoyi Xiong, Huiying Liu, and Yanwu Xu. Medsegdiff: Medical image segmentation with diffusion probabilistic model. In *Medical Imaging with Deep Learning*, pages 1623–1639. PMLR, 2024. 3
- [43] Junde Wu, Wei Ji, Huazhu Fu, Min Xu, Yueying Jin, and Yanwu Xu. Medsegdiff-v2: Diffusion-based medical image segmentation with transformer. In *Proceedings of the AAAI Conference on Artificial Intelligence*, pages 6030–6038, 2024. 3
- [44] Wenxuan Wu, Zhongang Qi, and Li Fuxin. Pointconv: Deep convolutional networks on 3d point clouds. In *Proceedings of the IEEE/CVF Conference on Computer Vision and Pattern Recognition*, pages 9621–9630, 2019. 2, 7
- [45] Weijia Wu, Yuzhong Zhao, Mike Zheng Shou, Hong Zhou, and Chunhua Shen. Diffumask: Synthesizing images with pixel-level annotations for semantic segmentation using diffusion models. In *Proceedings of the IEEE/CVF International Conference on Computer Vision*, pages 1206–1217, 2023. 1
- [46] Xiaoyang Wu, Yixing Lao, Li Jiang, Xihui Liu, and Hengshuang Zhao. Point transformer v2: Grouped vector atten-

- tion and partition-based pooling. *Advances in Neural Information Processing Systems*, 35:33330–33342, 2022. 1, 2, 6, 7
- [47] Xiaoyang Wu, Li Jiang, Peng-Shuai Wang, Zhijian Liu, Xihui Liu, Yu Qiao, Wanli Ouyang, Tong He, and Hengshuang Zhao. Point transformer v3: Simpler, faster, stronger. *arXiv preprint arXiv:2312.10035*, 2023. 6, 7
- [48] Zijie Wu, Yaonan Wang, Mingtao Feng, He Xie, and Ajmal Mian. Sketch and text guided diffusion model for colored point cloud generation. In *Proceedings of the IEEE/CVF International Conference on Computer Vision*, pages 8929–8939, 2023. 1, 3, 6, 7
- [49] Jiarui Xu, Sifei Liu, Arash Vahdat, Wonmin Byeon, Xiaolong Wang, and Shalini De Mello. Open-vocabulary panoptic segmentation with text-to-image diffusion models. In *Proceedings of the IEEE/CVF Conference on Computer Vision and Pattern Recognition*, pages 2955–2966, 2023. 1, 3
- [50] Mutian Xu, Runyu Ding, Hengshuang Zhao, and Xiaojuan Qi. Paconv: Position adaptive convolution with dynamic kernel assembling on point clouds. In *Proceedings of the IEEE/CVF Conference on Computer Vision and Pattern Recognition*, pages 3173–3182, 2021. 6, 8
- [51] Mutian Xu, Junhao Zhang, Zhipeng Zhou, Mingye Xu, Xiaojuan Qi, and Yu Qiao. Learning geometry-disentangled representation for complementary understanding of 3d object point cloud. In *Proceedings of the AAAI Conference on Artificial Intelligence*, pages 3056–3064, 2021. 2
- [52] Yunfan Ye, Kai Xu, Yuhang Huang, Renjiao Yi, and Zhiping Cai. Diffusionedge: Diffusion probabilistic model for crisp edge detection. *arXiv preprint arXiv:2401.02032*, 2024. 5
- [53] Li Yi, Vladimir G Kim, Duygu Ceylan, I-Chao Shen, Mengyan Yan, Hao Su, Cewu Lu, Qixing Huang, Alla Sheffer, and Leonidas Guibas. A scalable active framework for region annotation in 3d shape collections. *ACM Transactions on Graphics*, 35(6):1–12, 2016. 2, 6
- [54] Jiakang Yuan, Bo Zhang, Xiangchao Yan, Botian Shi, Tao Chen, Yikang Li, and Yu Qiao. Ad-pt: Autonomous driving pre-training with large-scale point cloud dataset. *Advances in Neural Information Processing Systems*, 36, 2024. 1
- [55] Hengshuang Zhao, Li Jiang, Chi-Wing Fu, and Jiaya Jia. Pointweb: Enhancing local neighborhood features for point cloud processing. In *Proceedings of the IEEE/CVF Conference on Computer Vision and Pattern Recognition*, pages 5565–5573, 2019. 2
- [56] Hengshuang Zhao, Li Jiang, Jiaya Jia, Philip HS Torr, and Vladlen Koltun. Point transformer. In *Proceedings of the IEEE International Conference on Computer Vision*, pages 16259–16268, 2021. 2, 3, 6, 7, 8
- [57] Xiao Zheng, Xiaoshui Huang, Guofeng Mei, Yuenan Hou, Zhaoyang Lyu, Bo Dai, Wanli Ouyang, and Yongshun Gong. Point cloud pre-training with diffusion models. In *Proceedings of the IEEE/CVF Conference on Computer Vision and Pattern Recognition*, pages 22935–22945, 2024. 3, 6
- [58] Xin-Yang Zheng, Hao Pan, Peng-Shuai Wang, Xin Tong, Yang Liu, and Heung-Yeung Shum. Locally attentional sdf diffusion for controllable 3d shape generation. *ACM Transactions on Graphics*, 42(4):1–13, 2023. 1
- [59] Linqi Zhou, Yilun Du, and Jiajun Wu. 3d shape generation and completion through point-voxel diffusion. In *Proceedings of the IEEE/CVF International Conference on Computer Vision*, pages 5826–5835, 2021. 1